Permeability estimation from digital rock images segmented through deep learning

Vivian C. Rodrigues[1], Maira C. O. L. Santo[1], Elizabeth M. B. D. Pontedeiro[1], José L. D. Alves[1], Leonardo Coelho[2], Paulo Couto[1]

[1]*Dept. of Civil Engineering, Federal University of Rio de Janeiro*
Centro de Tecnologia, 21941-972, Rio de Janeiro/RJ, Brazil
academica@coc.ufrj.br, coordpec@coc.ufrj.br
[2]*Dept. of Geology, Federal University of Rio de Janeiro*
Centro de Ciências Matemáticas e da Natureza, 21941-916, Rio de Janeiro/RJ, Brazil
graduacao@geologia.ufrj.br

Abstract. An accurate estimate of permeability is very important for the development and management of petroleum reservoirs. Knowledge of petrophysical properties is essential toachieve profi tability in production in the oil and gas (O&G) industry. Modeling of fl ow properties at pore scales has gained great prominence in oil industry projects with theadvances achieved with digital transformation. From digital images of reservoir rocks, it is possible to extract information from the porous system, in order to obtain petrophysicalproperties such as porosity, permeability, and, make suitable the comprehension of the connectivity of this system. The feasibility of acquiring three-dimensional images of theserocks, the industry began to use machine learning tools to assist the rock characterizations, thus, the entire modeling process is more efficient. And with high-performance computers, both the optimization and expansion of pore network have led to increasingly real flow calculations, which contributes to the knowledge of these properties. Theobjective of this research is to estimate the absolute permeability of rocks using micro tomography (microCT) images segmented using deep learning. It was used 12 samples of coquinas from the Morro do Chaves formation (Sergipe-Alagoas Basin) and these samples are similar to those from the Itapema formation (Santos Basin). The images have 42-micron resolution. Data were separated into training, validation and testing. Each batch of training images has 32 sub-images with 64x64 pixels ('patch') and the stride ratio equal to 1. It was used 100 learning epochs with an early stopping criterion. The model used for segmentation was U-net convolutional neural network with cross entropy as cost function and Adadelta (Zeiler [1]) optimization algorithm. Additionally, sensitivities were made regarding the use or not of the data augmentation technique and also regarding the use of input images with and without denoising filters. Deep learning models were generated in the Dragonfly program (Comet [2]) and the modeling of the pore network, using the PNM algorithm (Pore Network Modeling).

Keywords: Machine learning, Deep learning, Digital rock, PNM, Permeability

1 Introduction

A rock reservoir is a porous netework with enough permeability to allow fluids to flow sufficiently to fill its voids. The movement of these fluids is influenced by gravity and capillary forces, and when the flow is interrupted by a zone of low permeability, oil is formed in this trap (Peters [3]).

Physically, any buried sedimentary, igneous, or metamorphic rock that meets the conditions to petroleum accumulation can be used as a hydrocarbon reservoir. However, most of these reservoir are sedimentary (sandstone and carbonate).

Petrophysics is the study of the properties of rock and its interactions with fluids (gases, liquid hydrocarbons and aqueous solutions). This discipline provides basic understanding of the physical properties of permeable geological rocks and their interactions with the various fluids at the interstitial surface with an emphasis on the properties of rocks for single and multi-phase flows.

Among the petrophysical properties, there are porosity, absolute and relative permeability, water saturation, capillary pressure, wettability, etc (Peters [3]). The focus of this work is absolute permeability.

The permeability of a porous media is a measure of its ability to be crossed by fluids. In other words, per-

meability is a measure of the fluid conductivity of a material. By analogy with electrical conductors, permeability represents the inverse of the resistance that the material offers to the flow of fluids (Rosa et al. [4]). In addition to being one of the most important properties in porous media, it is determined by morphological characteristics such as tortuosity, porosity and connectivity (Zhang et al. [5]).

The large amount of data available in the O&G industry has made data-driven machine learning (*ML*) the first candidate for determining these properties (Tembely et al. [6]).

Digital images of pore-scale rocks are usually obtained through microtomography images that are segmented into voids and grains. (Elmorsy et al. [7]) An alternative to LBM is pore network modeling (PNM) which idealizes the complex network of pores in pores bodies and throats.

The determination of the absolute permeability of rocks from segmented digital images through deep learning is the object of this research.

2 Physical problem to be evaluated

The flow of fluids in porous media was formulated by Henry Darcy, in 1856, when studying water treatment problems through sand filters (see Figure 1). (Rosa et al. [4]) This equation, when adapted to express the flow of viscous fluids, can be expressed as follows: "The flow rate through a porous media is proportional to the area open to the flow and the pressure differential, and inversely proportional to the length and viscosity".

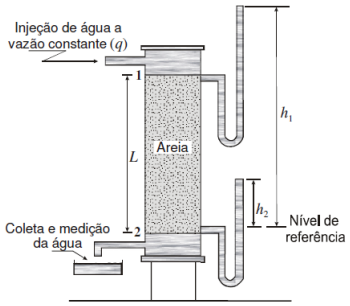

Figure 1. Darcy experiment (Rosa et al. [4])

For horizontal flow the flowrate equation is written as

$$q = \frac{kA\Delta P}{\mu L} \tag{1}$$

Enhanced oil recovery (EOR) techniques are directly impacted by accurate descriptions and characterizations of reservoirs that depend on prediction routines of their properties. (Tembely et al. [6]) Efficiency in determining petrophysical properties is critical for characterizing reservoirs and putting them into production.

2.1 Samples

The main types of reservoirs are associated with turbidite sandstones and carbonate environments. Takayama [8] presents the interpretation of GPR (*Ground Penetration Radar*) data in a carbonate quarry loacated at Sergipe-Alagoas Basin, specifically the Morro das Chaves formation, which is a coquina unit related, lithostratigraphically, to the West African and Campos basis.

According to Rocha et al. [9], the coquinas of the Itapema Formation (Barremiano/Aptiano, Santos Basin) are carbonate rocks interpreted in the literature as of lacustrine origin, and generally present heterogeneous deposits, from a sedimentological and diagenetic point of view, characterized by great faciological diversity and variability of their porous system.

In the present research it was used 12 samples of coquinas from the Morro do Chaves formation (Sergipe-Alagoas Basin), which are similar to those from the Itapema formation (pre-salt Santos Basin).The images have 42-micron resolution.

2.2 Deep learning model

In computer vision, segmentation refers to the process of dividing a digital image into multiple regions (set of pixels) or objects in order to simplify its representation and facilitate its quantification analysis. Is the task of classifying each pixel in an image from a predefined set of classes.

It was used a Deep Learning tool in Dragonfly software (Comet [2]) that provides deep models that are suitable for binary and multi-class semantic segmentation.

Datasets. It was used 12 datasets where 10 samples were considered for training set and the remaining 2 samples for test set.

Table 1. Digital rock samples for training and test set - 42 microns resolution

Class	Identification	ϕ[%]	k[md]	Set
RT1	105.3	9.7	2.7	Train
RT1	113.7	8.7	0.4	Train
RT1	146.25	4.0	0.04	Train
RT2	80	16.3	24.1	Train
RT2	126.05	13.0	13.0	Train
RT3	98.55	18.4	649.9	Train
RT3	187.95	12.1	152.4	Train
RT4	93	19.8	232.9	Train
RT4	94.4	18.5	103.4	Train
RT5	90.95	15.2	428.5	Train
RT1	173.5	10.8	5.16	Test
RT3	80.95	19.6	504.4	Test

The values of porosity and permeability are from routine laboratory petrophics analysis.

Model architecture. Semantic segmentation of an image was desired from biomedical image processing to output a class label to be assigned to each pixel. In Ronneberger et al. [10] it was proposed a modification of "fully convolutional network" called U-Net. The main idea of fully convolutional network is to supplement a usual contracting network by successive layers, where pooling operators (image feature detector of neural network convolutional layer and it decreases output image resolution) are replaced by upsampling operators. Hence trese layers increase the resolution of the output. The contracting path are combined with upsampled output in order to localize high resolution features.

In U-net architecture a modification of the upsampling part was proposed by the use of large number of feature channel, which allows the network to propagate context information to high resolution layers. As a consequence, the expansive path is more or less symmetric to the contracting path, and yields a u-shaped architecture (see figure 2). The network does not have a fully connected layers thus the segmentation map only contains the pixels for which the full context is available in the input image (Ronneberger et al. [10])

Cost function. The energy function is computed by a pixel-wise softmax over the final feature map combined with the cross entropy loss function. The soft-max is defined as $p_k(\mathbf{x}) = \exp(a_k(\mathbf{x}) / \left(\sum_{k'=1}^{K} \exp(a_{k'}(\mathbf{x})\right)$ where $a_k(\mathbf{x})$ denotes the activation feature channel k at pixel position $\mathbf{x} \in \Omega$ with $\Omega \subset \mathbb{Z}^2$. K is the number of classes and $p_k(\mathbf{x})$ is the approximated maximum-function (Ronneberger et al. [10]). I.e. $p_k(\mathbf{x}) \approx 1$ for the k that has the maximum activation $a_k(\mathbf{x})$ and $p_k(\mathbf{x}) \approx 0$ for all other k.

The cross entropy then penalizes at each position the deviation o $p_{l(\mathbf{x})}(\mathbf{x})$ from 1 using

$$E = \sum_{\mathbf{x} \in \mathbf{\Omega}} w(\mathbf{x}) \log(p_{l(\mathbf{x})}(\mathbf{x})) \tag{2}$$

where $l : \Omega \to \{1, \ldots, K\}$ is the true label of each pixel and $w : \Omega \to \mathbb{R}$ is a weight map that we introduce to give some pixels more importance in the training.

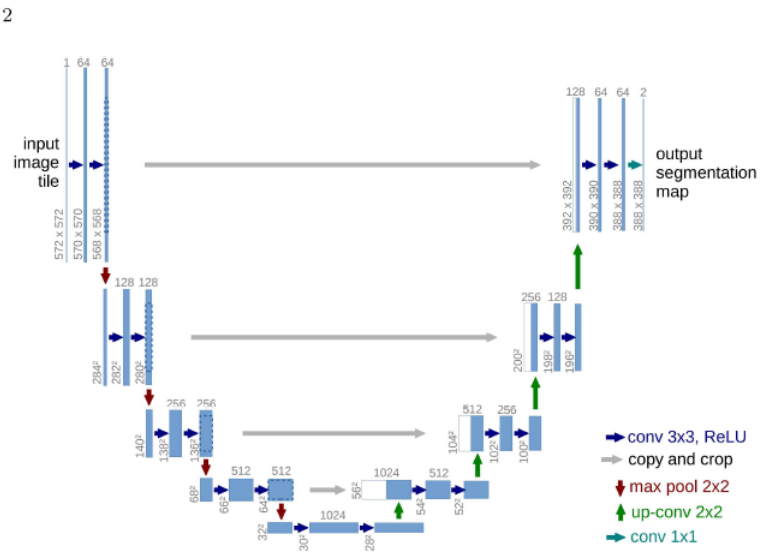

Figure 2. U-net architecture (example for 32x32 pixels in the lowest resolution) as per Ronneberger et al. [10]

Optimization Algorithm. For the learning algorithm it was considered the adaptative learning rate for gradient descent called Adadelta (Zeiler [1]). The method dynamically adapts over time using only the first order information and requires no manual tuning of the leaning rate. Instead of accumulating the sum of squared gradient over all time, the method retricts the window of past gradients that are accumulated to be some fixed size t. This ensures that learning continues to make progress even after many iterations of updates have been done. In Zeiler [1] is also proposed a correction of units with Hessian approximation by rearranging Newtons's Method (assuming a diagonal Hessian) for the inverse of second derivative to determine the quantities involved.

Models. The separation border is computed using morphological operations. The weight map is then computed as

$$w(\mathbf{x}) = w_c(\mathbf{x}) + w_0 \cdot \exp\left(-\frac{(d_1(\mathbf{x}) + d_2(\mathbf{x}))^2}{2\sigma^2}\right) \tag{3}$$

where $w_c : \Omega \to \mathbb{R}$ is the weight map to balance the class frequencies, $d_1 : \Omega \to \mathbb{R}$ denotes the distance to the border of the nearest cell and $d_2 : \Omega \to \mathbb{R}$ the distance to the border of the second nearest cell. In Ronneberger et al. [10] it was set $w_0 = 10$ and $\sigma \approx 5$ pixels.

For this paper the data was separated into training, validation and testing. Each batch of training images has 32 sub-images with 64x64 pixels ('patch') and the stride ratio equal to 1. It was used 100 learning epochs (single pass over all data patches) with an early stopping criterion.

For the training phase it was considered 4 models:

Table 2. Deep learning tool parameters

Model	Train dataset(TD)	Data augmentation	% of TD for validation
A	Filtered images	Yes	15
B	Filtered images	No	10
C	Original images	Yes	15
D	Original images	No	10

For each test sample (see Table 1) it was generated a segmentation based on trained models. The best two results of segmentation were selected for each test sample for PNM analysis.

2.3 Pore network modelling

In PNM, instead of solving partial differential equations of order n (PDEs), the pore space is treated as a network of "pipes". Transport inside the network is modeled using finite difference schemes to solve 1D analytical solutions of the relevant transport equations. Despite this simplification, this type of simulation can efficiently predict several aspects of multiphase transport. The dimensions and connectivity of the pores and throats are adjusted to agree with the known physical structure. The structural properties of the porous material can be obtained from imaging techniques or artificially generated by a computer. PNMs are naturally geared toward percolation calculations, so they simulate realistic fluid invasion processes with computational ease (Gostick et al. [11]).

Dragonfly has the OpenPNM extension as per Gostick et al. [12] and it was designed with three general objectives: accessibility to a wide audience, generality to as many applications as possible, and is extensible to simulate any type of physical process.

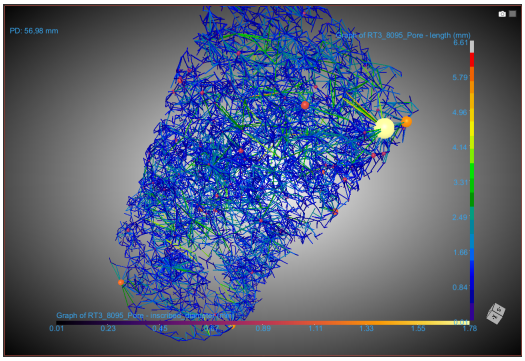

Figure 3. Pore network as per Gostick [13] from segmentation reference (RT3 80.93 ground truth-GT) in Dragonfly software (Comet [2]).

2.4 Results

Deep Learning - DL.The analysis were performed with 42 microns resolution images. The figure 4 presents the loss and validation loss of the four models used for segmentation learning.

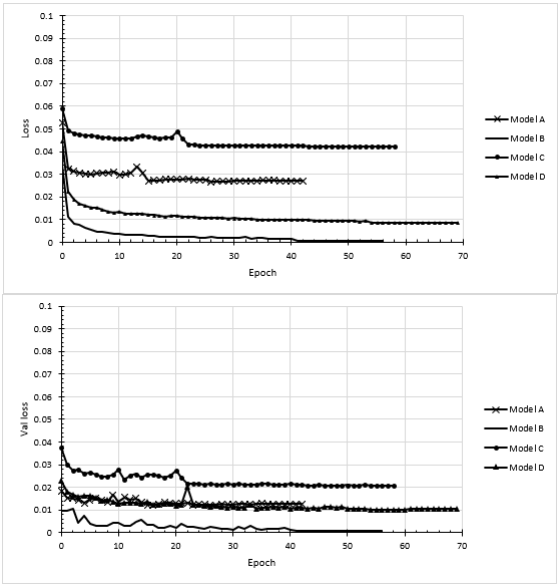

Figure 4. Loss and validation loss of deep models.

The selected models for each test sample are illustrated in figure 5 and figure 6. Note that the labeled green voxels represents the pore space, the light orange is the rock matrix and, thus the pink labeled voxels are the background.

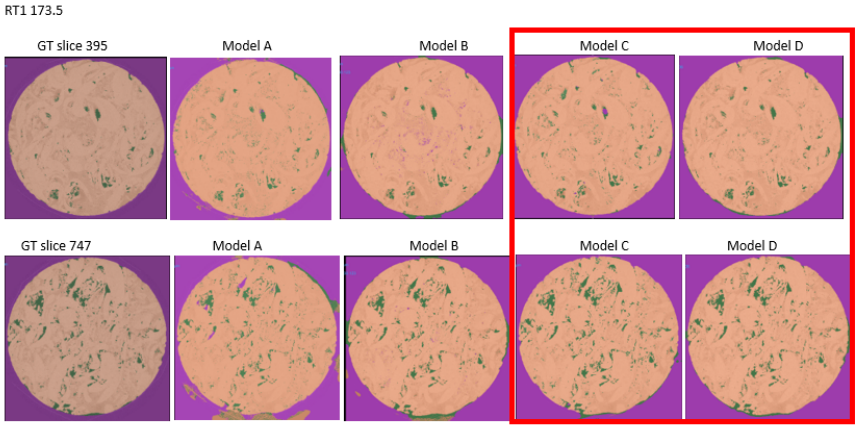

Figure 5. RT1 137.5 sample DL result. The selected models are highlighted in red (GT-ground truth).

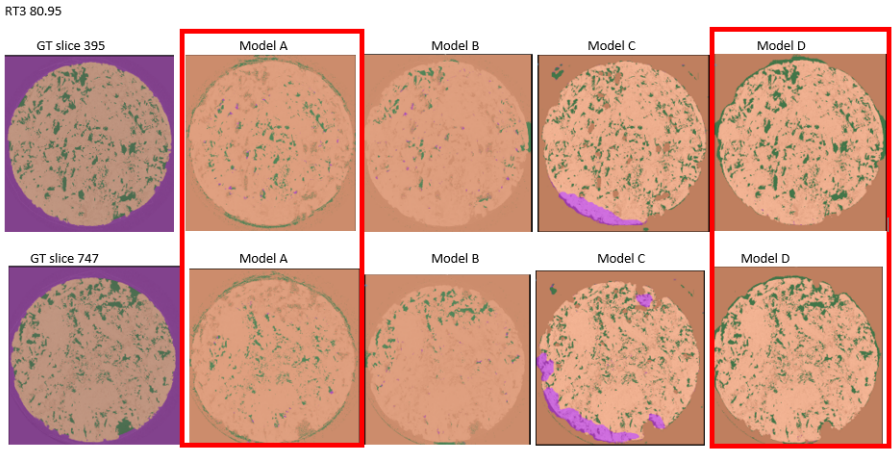

Figure 6. RT3 80.95 sample DL result. The selected models are highlighted in red (GT-ground truth).

Although RT3 80.95 sample background was not labelled correctly by the models, the pore space was better identified and this is the principal information for PNM analysis. Thus, the fact that the rock matrix and background voxels were not correctly differentiated did not impact the pore network modeling.

PNM.The results of pore network modeling are summarized in the table 3. Note that is presented the porosity (ϕ) and absolute permeability (k) calculations of ground truth (GT) and 2 deep learning (DL) segmentation of each test sample. These values are compared to laboratory routine petrophysics ($rout$).

Table 3. PNM

Sample	ϕ[%]	ϕ_{GT}[%]	$\phi_{DL}1$[%]	$\phi_{DL}2$[%]	k_{GT}[mD]	k_{rout}[mD]	$k_{DL}1$[mD]	$k_{DL}2$[mD]
RT1 173.5	3.0	10.8	4.9	4.6	0.5	5.2	0.01	0.3
RT3 80.95	15.5	19.6	8.8	17.0	669.1	504.4	1595.8	4122.38

Note that for sample RT1 173.5 results 1 and 2 correpond to models C and D respectvely. The same is applied to sample RT3 80.95. In addition it was considered the rock matrix ground truth voxels to calculate DL porosities of RT3 80.95 sample.

3 Conclusions

Although final loss in figure 4 is a small value, the learning models still presented incorrect labelled pixels principally for sample RT3 80.95. This is justified by the balance of the training dataset that have more samples with lower porosity and permeability (see table 1).

Permeability calculations are still under evaluation but que higher values of deep learning results compared to petrophysics and ground truth is justified by labelled pixels as pore outside the sample RT3 80.95 (figure 6).

Thus, deep models had a better performance for sample with lower porosity and permeability and model D for RT1 173.5 presented the best result.

Acknowledgements. This research was carried out in association with the ongoing R&D project registered as ANP nº 23020-1, "Caracterização Experimental, Modelagem e Otimização de Processos de Injeção de Água Alternada Com Gás – WAG-EX Fase II" (UFRJ/Shell Brasil/ANP), sponsored by Shell Brasil Petróleo Ltda under the ANP R&D levy as "Compromisso de Investimentos com Pesquisa e Desenvolvimento".

The authors would like to acknowledge the support of the Human Resources Program of the National Agency of Petroleum, Natural Gas, and Biofuels – PRH-ANP, supported with resources from the investment of qualified oil companies under the R&D Clause of ANP Resolution No. 50/2015. Additionally, this study was financed, in part, by the São Paulo Research Foundation (FAPESP), Brasil. Process Number 2024/11460-7.

This study was also financed in part by the Coordenação de Aperfeiçoamento de Pessoal de Nível Superior – Brasil (CAPES) – Finance Code 001. The authors also acknowledge the partial support from the Conselho Nacional de Desenvolvimento Científico e Tecnológico - Brasil (CNPq) through the research productivity grant 310291/2022-4.

Authorship statement. The authors hereby confirm that they are the sole liable persons responsible for the authorship of this work, and that all material that has been herein included as part of the present paper is either the property (and authorship) of the authors, or has the permission of the owners to be included here.

References

[1] M. D. Zeiler. ADADELTA: an adaptive learning rate method. *CoRR*, vol. abs/1212.5701, 2012.

[2] Comet. Dragonfly (commercial software). Eletronic. https://dragonfly.comet.tech/, 2015.

[3] E. J. Peters. *Petrophysics*. Department of Petroleum and Geosystem Engineering. The University of Texas Austin USA 78712, Texas, 1 edition, 2006.

[4] A. J. Rosa, de R. Souza Carvalho, and J. A. D. Xavier. *Engenharia de reservatórios de petróleo*. Interciência, Rio de Janeiro, 1 edition, 2006.

[5] H. Zhang, H. Yu, X. Yuan, H. Xu, M. Micheal, J. Zhang, H. Shu, G. Wang, and H. Wu. Permeability prediction of low-resolution porous media images using autoencoder-based convolutional neural network. *Journal of Petroleum Science and Engineering*, vol. 208, pp. 109589, 2022.

[6] M. Tembely, A. M. AlSumaiti, and W. S. Alameri. Machine and deep learning for estimating the permeability of complex carbonate rock from x-ray micro-computed tomography. *Energy Reports*, vol. 7, pp. 1460–1472, 2021.

[7] M. Elmorsy, W. El-Dakhakhni, and B. Zhao. Generalizable permeability prediction of digital porous media via a novel multi-scale 3d convolutional neural network. *Water Resources Research*, vol. 58, n. 3, pp. e2021WR031454. e2021WR031454 2021WR031454, 2022.

[8] P. Takayama. 3d gpr geophysics modeling in carbonate reservoirs analogues applying geometric attributes: Coqueiro seco formation sergipe-alagoas basin. mathesis, Universidade Estadual do Rio de Janeiro, 2008.

[9] L. Rocha, J. Favoreto, and L. Borghi. Coquinas da formação itapema, campo de mero (pré-sal da bacia de santos): Análise de microfácies e paleoambiente deposicional. *Anuário do Instituro de Geociências*, vol. 44, 2021.

[10] O. Ronneberger, P. Fischer, and T. Brox. U-net: Convolutional networks for biomedical image segmentation. In N. Navab, J. Hornegger, W. M. Wells, and A. F. Frangi, eds, *Medical Image Computing and Computer-Assisted Intervention – MICCAI 2015*, pp. 234–241, Cham. Springer International Publishing, 2015.

[11] J. Gostick, M. Aghighi, J. Hinebaugh, T. Tranter, M. A. Hoeh, H. Day, B. Spellacy, M. H. Sharqawy, A. Bazylak, A. Burns, W. Lehnert, and A. Putz. Openpnm: A pore network modeling package. *Computing in Science & Engineering*, vol. 18, n. 4, pp. 60–74, 2016.

[12] J. T. Gostick, Z. A. Khan, T. G. Tranter, M. D. Kok, M. Agnaou, M. Sadeghi, and R. Jervis. Porespy: A python toolkit for quantitative analysis of porous media images. *Journal of Open Source Software*, vol. 4, n. 37, pp. 1296, 2019.

[13] J. T. Gostick. Versatile and efficient pore network extraction method using marker-based watershed segmentation. *Phys. Rev. E*, vol. 96, pp. 023307, 2017.